diversity

MDPI

Article

New Mitogenomes of the *Harnischia* Generic Complex (Diptera: Chironomidae) and Their Implication in Phylogenetics

Wenbin Liu [1,2], Yaning Tang [2], Jiaxin Nie [2], Haoran Yan [3], Wentao Liang [1,4], Yanfei Zhang [1,4] and Chuncai Yan [2,*]

[1] Yinshanbeilu Grassland Eco-Hydrology National Observation and Research Station, China Institute of Water Resources and Hydropower Research, Beijing 100038, China; skylwb@tjnu.edu.cn (W.L.)
[2] Tianjin Key Laboratory of Conservation and Utilization of Animal Diversity, Tianjin Normal University, Tianjin 300387, China
[3] M-Grass Ecology and Environment (Group) Co., Ltd., Hohhot 010050, China
[4] Institute of Water Resource for Pastoral Area, Ministry of Water Resources of the People's Republic of China, Hohhot 010020, China
* Correspondence: skyycc@tjnu.edu.cn

Abstract: The *Harnischia* generic complex, a significant assemblage within the tribe Chironomini, extensive global sampling and the integration of multi-characteristic data for comprehensive analysis are essential to elucidate the phylogenetic relationships within the *Harnischia* generic complex. We sequenced, assembled, and annotated the mitochondrial genomes of a single species each from the genera *Parachironomus* Lenz, *Robackia* Saether and *Saetheria* Jackson. Additionally, we incorporated 26 previously published mitogenomes into our analysis to delve deeper into the characteristics of these mitogenomes. Our findings indicate the close affinity between (*Cryptochironomus* + *Demicryptochironomus*) and (*Harnischia* + *Microchironomus*), aligning consistently with previous research outcomes showing that the *Harnischia* generic complex and *Chironomus* are phylogenetically close, and their clade forms a sister group with the *Polypedilum* generic complex. Based on mitochondrial genome data, *Robackia* is identified as the basal taxon being relatively primitive, with *Parachironomus* and *Saetheria* also appearing as primitive within the complex.

Keywords: Chironominae; mitogenome; phylogenomics; *Harnischia*

check for updates

Academic Editor: Luc Legal

Received: 2 January 2025
Revised: 27 January 2025
Accepted: 27 January 2025
Published: 29 January 2025

Citation: Liu, W.; Tang, Y.; Nie, J.; Yan, H.; Liang, W.; Zhang, Y.; Yan, C. New Mitogenomes of the *Harnischia* Generic Complex (Diptera: Chironomidae) and Their Implication in Phylogenetics. *Diversity* **2025**, *17*, 96. https://doi.org/10.3390/d17020096

1. Introduction

Chironomidae, a diverse family of freshwater flies, are unparalleled in their ability to inhabit a wide range of aquatic environments, from low-oxygen waters to the icy heights of the Himalayas and the abyssal depths of Lake Baikal [1]. Their resilience in extreme conditions, such as temperatures as low as −16 °C, and their status as one of the most geographically widespread insects, make them invaluable bioindicators for ecological health and environmental change [2,3]. These aquatic insects, with an estimated 15,000 species globally, exhibit remarkable species diversity attributed to their antiquity, limited dispersal, and evolutionary plasticity [1]. They play a pivotal role in aquatic ecosystems, contributing significantly to detritus processing and trophic dynamics, while their tolerance to extreme conditions renders them valuable for ecological and water quality assessments [4]. Additionally, their high population densities and life cycle characteristics are central to theoretical ecological studies and have practical implications for biological monitoring and as a food resource for various animals [5,6].

The Chironomidae family is currently classified into 11 subfamilies within the global taxonomy system [7,8]. Among these, the Chironominae subfamily stands out as one of

the largest within the Chironomidae family [9,10]. Sæther (1977) conducted a phylogenetic study on the Chironominae based on characteristics of female adults, proposing for the first time a division into three tribes: Chironomini, Pseudochironomini, and Tanytarsini. He also suggested that the Chironomini is a monophyletic group, which was a significant contribution to the understanding of the family's evolutionary relationships [11].

The *Harnischia* generic complex, a significant assemblage within the tribe Chironomini, comprises over 320 species across 20 genera worldwide [12,13]. Due to their broad distribution, high population densities, and significant biological mass, coupled with a high degree of habitat diversity, the composition and community structure of *Harnischia* reflect long-term changes in aquatic environments [14]. Consequently, this group has long been recognized as a crucial indicator in environmental monitoring and is extensively utilized in the biological assessment and evaluation of water quality [14]. The concept of the *Harnischia* generic group was first introduced in 1969 [15]. In 1945, Townes contributed significantly to the study of the *Harnischia* generic complex by distinguishing it into two genera, *Harnischia* and *Cryptochironomus*, through his revision of the male adults of the tribe Chironomini in North America [16]. Then, Sæther's research significantly contributed to the systematic revision of the *Harnischia* generic group on a global scale, establishing nine new generic taxa and conducting a preliminary exploration of the phylogenetic relationships among these genera based on morphological characteristics [11,17]. This work supported the hypothesis that the *Harnischia* generic group is monophyletic within the Chironomidae family [17].

Phylogenetic research on the *Harnischia* generic complex has historically been underdeveloped, with contentious boundaries and taxonomic statuses of its genera, including the presence of monotypic genera [14]. This has, to a certain extent, impeded systematic phylogenetic studies within the Chironominae subfamily [17]. Previous studies, constrained by limited morphological traits or short molecular sequences and regionally confined sampling, have resulted in numerous conflicting hypotheses due to the incompleteness of samples and characteristics [14]. Therefore, extensive global sampling and the integration of multi-characteristic data for comprehensive analysis are essential to elucidate the phylogenetic relationships within the *Harnischia* generic complex, thereby fostering advancements in the phylogenetic research of the Chironomidae family [18].

Mitochondrial genomes, abbreviated as mtDNA, represent the DNA molecules resident within cellular mitochondria [19,20]. Insect mitochondrial genomes, typically exhibiting a double-stranded circular structure ranging in size from 14 to 20 kilobases (kb), are responsible for encoding a subset of mitochondrial proteins, as well as mitochondrial ribosomal RNA (rRNA) and transfer RNA (tRNA) [21–23]. The unique properties of insect mt DNA, particularly its high variability among different species, provide invaluable genetic markers for investigating insect classification, phylogenetic relationships, and adaptive evolution [24,25]. Characterized by maternal inheritance, low recombination rates, and rapid evolution, these genomes serve as pivotal tools in molecular systematics, population genetics, species identification, and evolutionary studies [26,27]. In recent years, the enhancement of sequencing technologies and the refinement of analytical approaches have facilitated the extensive application of mitochondrial genomes in the fields of phylogenetics and species identification, particularly within the order Diptera and the family Chironomidae [28–31].

Parachironomus Lenz, 1921, *Robackia* Saether, 1977, and *Saetheria* Jackson, 1977 are three key genera in the *Harnischia* generic complex, yet their mitochondrial genomes remain undescribed in the scientific literature, highlighting a significant gap in our understanding of these taxonomically important groups. The genus *Parachironomus* Lenz, 1921, is globally distributed with at least 30 species from the Holarctic region, a distribution complicated by synonymy issues and tentative species assignments that hinder precise estimations,

and these larvae exhibit versatile ecological adaptation, being found in both standing and flowing waters [32,33]. *Robackia* Saether, 1977, and *Saetheria* Jackson, 1977, two genera with a modest number of species within the *Harnischia* generic complex, are characterized by their larvae which thrive in the sandy substrates of lakes and streams, significantly contributing to the aquatic ecosystem as integral members of the benthos community [17,32].

To comprehend the relationships among the three genera *Parachironomus* Lenz, *Robackia* Saether, and *Saetheria* Jackson within the *Harnischia* complex, to investigate the position of the *Harnischia* complex within the subfamily Chironominae, and to explore the characteristics of the mitochondrial genomes of species related to the *Harnischia* complex. In this study, we sequenced, assembled, and annotated the mitochondrial genomes of a single species each from the genera *Parachironomus* Lenz, *Robackia* Saether and *Saetheria* Jackson. Additionally, we incorporated 26 previously published mitogenomes into our analysis to delve deeper into the characteristics of these mitogenomes. Utilizing Bayesian Inference (BI) and Maximum Likelihood (ML) methods across various databases, we reconstructed the phylogenetic relationships among the subfamily Chironominae, drawing insights from an analysis of 29 mitochondrial genomes. Our findings indicate the sister-group relationship between *Cryptochironomus* and *Demicryptochironomus*. Furthermore, our analysis also confirms the close affinity between (*Cryptochironomus* + *Demicryptochironomus*) and (*Harnischia* + *Microchironomus*), aligning consistently with previous research outcomes the *Harnischia* generic complex and *Chironomus* are phylogenetically close, and their clade forms a sister group with the *Polypedilum* generic complex. Based on mitochondrial genome data, *Robackia* is identified as the basal taxon, which is relatively primitive, with *Parachironomus* and *Saetheria* also appearing as primitive within the complex.

2. Materials and Methods

2.1. Sampling and Sequencing

Samples of *Robackia demeijerei* (Kruseman, 1933) and *Saetheria tamanipparai* (Sasa, 1983) were collected from Huanghuagou Scenic Area, Wulanchabu City, Inner Mongolia Autonomous Region of China (112°52′91″ E, 41°13′30″ N) at 24 July 2018 by Wenbin Liu and *Parachironomus demissum* (Yan, Wang and Bu, 2012) from Aibugai River, Darhan Muminggan United Banner, Baotou City, Inner Mongolia Autonomous Region of China (110°26′30″ E, 41°42′01″ N) at 14 August 2023 by Haoran Yan. Species identification is predicated on a comprehensive dual methodology that integrates both morphological evaluation and barcode sequence analysis. The morphological characteristics of the two species under scrutiny conform to the descriptions provided in references [34–37]. Genomic DNA was meticulously extracted from thoracic and pedal tissues using the Qiagen DNeasy Blood and Tissue Kit at Tianjin Normal University (TJNU), Tianjin, China, following a rigorously standardized protocol. Before proceeding with DNA extraction and morphological analysis, the specimens were preserved in a solution of 85% ethanol post-collection and stored at a temperature of −20 °C to ensure sample integrity. The voucher specimens were deposited in the College of Life Sciences at TJNU, Tianjin, China, for future reference and analytical studies.

To amplify the 658-bp segment of the mitochondrial cytochrome c oxidase subunit I (COI) barcode region, which is essential for species identification and subsequent mitochondrial genome assembly parameters, we employed the universal primers LCO1490 and HCO2198 [24,25]. The subsequent genomic sequencing was outsourced to Berry Genomics in Beijing, China, for next-generation sequencing. Employing the Illumina Truseq Nano DNA HT Sample Preparation Kit, we prepared sequencing libraries, which were optimized for subsequent analytical processes. DNA fragments with an insert size of 350 bp were

sequenced using the Illumina NovaSeq 6000 platform with a paired-end (PE150) strategy, thereby enhancing the efficiency of data generation.

The initial sequencing reads underwent stringent quality control, with Trimmomatic being utilized to refine and cleanse the data by removing sequences of poor quality and any associated artifacts. The high-quality, refined reads were then employed for subsequent bioinformatics analyses, as detailed in reference [38]. This process marked the initial phase in deciphering the genetic architecture and evolutionary relationships of the species under investigation.

2.2. Assembly, Annotation and Composition Analyses

To de novo assemble the mitogenome sequences, we employed NOVOPlasty v3.8.3, a software developed in Brussels, Belgium, using the COI barcode as the seed sequence. We systematically tested a variety of k-mer sizes ranging from 23 to 39 bp to refine the assembly process, as detailed in reference [39]. The annotation of the assembled mitogenome was conducted following the stringent guidelines provided in [24], ensuring the precise identification of functional elements. The secondary structure of tRNAs was carefully analyzed using the MITOS WebServer, which offers a comprehensive view of their conformational characteristics. For the annotation of rRNAs and Protein-Coding Genes (PCGs), we employed a hybrid approach. Initially, we utilized the Clustal Omega algorithm within Geneious for automated annotation, which was then subjected to manual refinement to enhance accuracy. Additionally, the Clustal W function within MEGA 11 was applied as a complementary verification step to refine the boundaries of rRNAs and PCGs, as described in references [40,41].

To gain insights into the nucleotide composition and biases within the mitogenome, we utilized SeqKit v0.16.0, a robust tool developed in Chongqing, China [42]. This analysis not only revealed the overall nucleotide composition but also the specific composition of individual genes. The mitogenome's visual representation was created using the CGView server, providing an intuitive and comprehensive overview of the genetic structure. To further investigate codon usage patterns, we employed MEGA 11 [43], which facilitated the calculation of nucleotide composition, codon usage, and relative synonymous codon usage. We also quantified nucleotide composition biases using AT-skew, defined as $(A - T)/(A + T)$, and GC-skew, calculated as $(G - C)/(G + C)$, offering insights into the evolutionary pressures that may be shaping the mitogenome. Finally, to elucidate the evolutionary dynamics of the mitogenome, we calculated synonymous (Ks) and non-synonymous substitution rates (Ka) using DnaSP6 [44]. This analysis provided insights into the selective pressures acting on the mitogenome, distinguishing between changes that alter amino acid sequences (non-synonymous) and those that do not (synonymous).

2.3. Phylogenetic Analyses

To delve into the phylogenetic positioning *Harnischia* generic complex, mitochondrial genome sequences of 29 registered Chironomidae species were retrieved from GenBank at NCBI. This comprehensive dataset encompassed 25 *subfamily* Chironominae species, two *Cricotopus* of subfamily *Orthocladiinae* and two Tanypus of subfamily Tanypodinae species were used as an outgroup (Table 1). For the phylogenetic analysis, a curated selection of 29 mitochondrial genomes was meticulously assembled, from which two ribosomal RNAs (rRNAs) and 13 Protein-Coding Genes (PCGs) were extracted. The alignment of these sequences was performed with precision using MAFFT, a software developed in Osaka, Japan, employing the L-INS-I method to eliminate ambiguous regions in both nucleotide and protein sequence alignments in a batch process. Post-alignment, Trimal v1.4.1, a tool

from Barcelona, Spain, was utilized to further refine the alignments by trimming, ensuring the data quality necessary for subsequent phylogenetic analyses.

We generated five distinct data matrices using FASconCAT-G v1.04, a software package from Santa Cruz, CA, USA, each designed to capture different facets of the genetic information: cds Matrix: This matrix includes all three codon positions of the 13 protein-coding genes (PCGs), providing a complete view of the coding region. cds_rna Matrix: This matrix broadens its scope to encompass both the 13 PCGs (covering all codon positions) and the two ribosomal RNAs (rRNAs), merging coding and non-coding components. cds12_rrna Matrix: This matrix specifically includes only the first and second codon positions of the PCGs along with the rRNAs, highlighting the most conserved areas within the coding genes. cds12 Matrix: Focusing on the initial and second codon positions of the 13 PCGs, this matrix emphasizes the evolutionary significance of these pivotal positions. cds_faa Matrix: By utilizing the amino acid sequences from the 13 PCGs, this matrix shifts the focus away from nucleotide-level differences and evaluates relationships at the protein level. To assess the heterogeneity among these diverse matrices, AliGROOVE v1.06, a software from Bonn, Germany, was engaged, leveraging insights from previous studies [45,46] as benchmarks. Following this, two phylogenetic trees were constructed: a Maximum Likelihood (ML) tree using IQ-tree v2.0.7 and a Bayesian Inference (BI) tree utilizing Phylobayes-MPI v1.8.

Table 1. Mitogenomes of the 27 species used in this study.

Subfamily	Species	GenBank Accession Number	Reference
Chironominae	*Parachironomus demissum*	Pending	This study
	Robackia demeijerei	Pending	This study
	Saetheria tamanipparai	Pending	This study
	Cladopelma edwardsi	PQ014460	[5]
	Cladopelma virescens	PQ014464	[5]
	Cryptochironomus maculus	PQ014454	[5]
	Cryptochironomus rostratus	PQ014455	[5]
	Demicryptochironomus minus	PQ014456	[5]
	Demicryptochironomus spatulatus	PQ014457	[5]
	Harnischia angularis	PQ014458	[5]
	Harnischia turgidula	PQ014459	[5]
	Chironomus anthracinus	ON975026	[47]
	Chironomus nipponensis	ON975028	[47]
	Microchironomus tener	ON975027	[47]
	Microchironomus tabarui	MZ261913	[48]
	Stenochironomus okialbus	OL753645	[49]
	Stenochironomus tobaduodecimus	OL753648	[49]
	Endochironomus albipennis	OP950227	[7]
	Endochironomus pekanus	OP950219	[7]
	Polypedilum yongsanensis	OP950222	[7]
	Polypedilum masudai	OK513041	[7]
	Stictochironomus akizukii	OP950218	[7]
	Stictochironomus juncaii	OP950226	[7]
	Microtendipes bimaculatus	PP966953	NCBI
	Microtendipes tuberosus	PP966949	NCBI
Orthocladiinae	*Cricotopus bicinctus*	OP006251	[29]
	Cricotopus dentatus	OP006255	[29]
Tanypodinae	*Tanypus chinensis*	PQ014462	[31]
	Tanypus kraatti	PQ014453	[31]

3. Results

The complete mitogenome of *Parachironomus demissum* was 15,804 bp, *Robackia demeijerei* was 16,218 bp, and *Saetheria tamanipparai* was 15,899 bp long. The typical double-stranded circular DNA molecule, characteristic of insect mitochondrial genomes, contains a total of 37 genes—including 13 protein-coding genes (PCGs), 22 tRNA genes, and two rRNA genes—as well as one control region, with the gene-coding strand following the standard arrangement. (Figure 1).

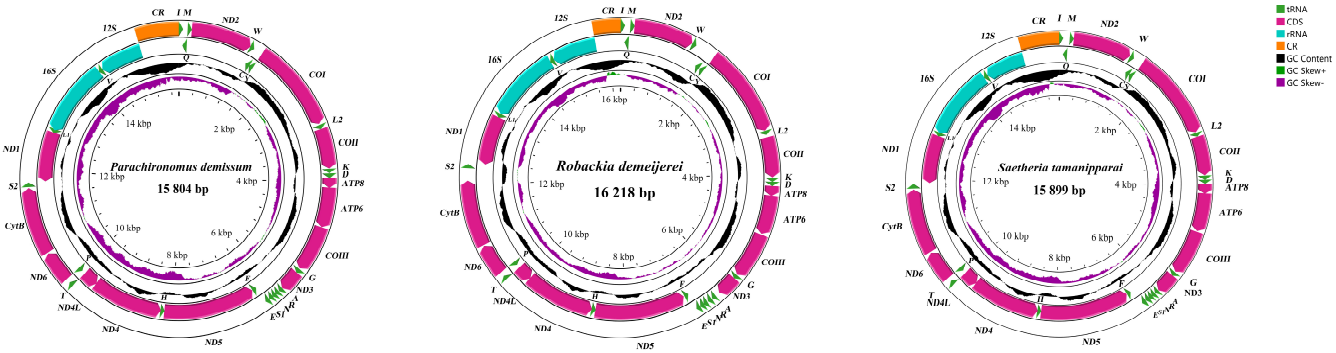

Figure 1. The mitogenome map delineates the distinct mitochondrial genome characteristics of various representative species across three genera within the *Harnischia* generic complex. The map uses arrows to denote gene transcription direction and employs standard abbreviations for PCGs and rRNAs, along with simplified tRNA notations, for clarity. The second circle displays GC content, revealing nucleotide composition, while the third circle shows GC-skew, highlighting structural asymmetry. The innermost circle summarizes mitogenome length, offering a holistic view of its attributes.

The genomic nucleotide composition of *Parachironomus demissum* shows a pronounced AT bias, with an overall AT content of 78.12%. The control region exhibits the highest AT content at 95.02%. The rRNAs have a higher AT content (84.09%) compared to protein-coding genes (76.78%). Within the protein-coding genes, *ND6* has the highest AT content at 85.39%, while *COX1* has the lowest at 68.68%. The AT content at the first and second codon positions of protein-coding genes is lower than at the third position, with values of 71.65% and 68.86%, respectively, compared to 89.84%. The mitochondrial genome sequence exhibits a slight A skew and a pronounced C skew. Initiation codons in the 13 protein-coding genes of the short whip gnat mitochondrial genome are predominantly ATN patterns (ATG, ATT, and ATC), with exceptions including *COX1* and *ND1* (TTG) and *ND5* (GTG). Termination codons are either incomplete (T in ND4) or complete (TAA in all others). The 22 tRNAs vary in length from 65 to 72 bp. The 16S rRNA is 1404 bp long with an AT content of 85.18%, and the 12S rRNA is 812 bp long with an AT content of 83.00%. The control region, at 723 bp, shows a slight T skew (−0.02) and a strong C skew (−0.33) (Table 2).

The genomic nucleotide composition of *Robackia demeijerei* was 41.61% A, 39.25% T, 7.96% C, and 11.18% G. The mitochondrial genome's base composition reveals a pronounced AT bias, with A + T comprising 80.86% of the total bases; the AT skew is 0.03 and the GC skew is −0.17, indicating a minor A skew and a significant C skew. The control region exhibits an exceptionally high AT content of 96.88%, the most abundant across all genomic regions. The rRNAs have an overall AT content of 86.13%, surpassing that of protein-coding genes. Among the 13 protein-coding genes, the collective AT content is 79.38%, with *ATP8* and *ND6* showing relatively high AT contents of 87.50% and 87.08%, respectively, while *COX3* has the lowest at 69.58%. The third codon position in protein-coding genes has a notably high AT content of 93.80%, significantly exceeding that of the first

(73.59%) and second (70.74%) positions. Initiation codons in most of the 13 protein-coding genes follow the ATN motif (ATG and ATT), with exceptions being *COX1* and *ND1*, which use TTG, and *ND5*, which uses GTG; all genes utilize the complete TAA as the termination codon. The lengths of the 22 canonical tRNAs vary from 65 to 72 bp, with the 16S rRNA spanning 1394 bp and an AT content of 86.66%. The 12S rRNA is 854 bp in length, with an AT content of 85.60%. The control region at 481 bp lacks a significant AT bias (Table 3).

Table 2. Nucleotide composition and skewness of mitogenomes of *Parachironomus demissum* (PCG: Protein-Coding Gene, CR: Control Region).

Gene Type	Length (bp)	Base Composition (%)						Skew	
		A	T	C	G	A + T	G + C	AT-Skew	GC-Skew
Whole genome	16,266	39.61	36.27	14.55	9.57	75.88	24.12	0.044	−0.206
PCG	11,216	31.28	42.73	13.45	12.54	74.00	26.00	−0.155	−0.035
PCG 1st codon position	3740	31.96	36.47	12.22	19.35	68.43	31.57	−0.066	0.226
PCG 2nd codon position	3738	20.99	45.57	19.93	13.51	66.56	33.44	−0.369	−0.192
PCG 3rd codon position	3738	40.87	46.15	8.21	4.77	87.03	12.98	−0.061	−0.265
ATP6	678	32.45	41.00	15.63	10.91	73.45	26.54	−0.116	−0.178
ATP8	168	42.86	39.88	12.50	4.76	82.74	17.26	0.036	−0.448
COX1	1534	28.68	37.87	17.67	15.78	66.55	33.45	−0.138	−0.057
COX2	688	35.03	37.79	15.12	12.06	72.82	27.18	−0.038	−0.113
COX3	789	30.54	36.88	17.74	14.83	67.42	32.57	−0.094	−0.089
CYTB	1137	32.63	37.03	17.77	12.58	69.66	30.35	−0.063	−0.171
ND1	948	24.58	49.05	9.07	17.30	73.63	26.37	−0.332	0.312
ND2	1026	32.46	45.42	12.87	9.26	77.88	22.13	−0.166	−0.163
ND3	354	31.07	41.81	16.38	10.73	72.88	27.11	−0.147	−0.208
ND4	1341	28.34	47.35	8.58	15.73	75.69	24.31	−0.251	0.294
ND4L	294	27.55	52.04	6.80	13.61	79.59	20.41	−0.308	0.334
ND5	1734	28.43	45.50	9.69	16.38	73.93	26.07	−0.231	0.257
ND6	525	34.48	46.48	12.19	6.86	80.96	19.05	−0.148	−0.280
All rRNA	2202	37.30	42.91	6.73	13.07	80.21	19.79	−0.070	0.320
12S	807	36.68	42.38	7.43	13.51	79.06	20.94	−0.072	0.290
16S	1395	37.92	43.44	6.02	12.62	81.36	18.64	−0.068	0.354
CR	952	47.16	43.59	7.14	2.10	90.75	9.24	0.039	−0.545

In the *Saetheria tamanipparai* mitochondrial genome, the base composition is characterized by A = 39.91%, T = 39.20%, G = 8.40%, and C = 12.50%, resulting in an A + T percentage of 79.11%, which demonstrates a significant AT bias. The AT skew is minimal at 0.01, while the GC skew is more pronounced at −0.20, indicating a subtle A skew and a marked C skew. The control region reaches an AT content peak of 96.00%. The rRNAs have a higher overall AT content of 85.70% compared to protein-coding genes. Among the 13 protein-coding genes, the collective AT content is 77.40%, with *ND6* showing the highest at 85.76% and *COX3* the lowest at 68.95%. The third codon position in protein-coding genes has an exceptionally high AT content of 90.18%, significantly exceeding that of the first (72.54%) and second (69.46%) positions. Initiation codons in the mitochondrial genome's protein-coding genes predominantly follow the ATN pattern (ATG, ATT, and ATC), with exceptions including *COX1* and *ND1* (TTG) and *ND5* (GTG). Termination codons uniformly employ the canonical TAA. The 22 tRNA genes vary in length from 65 to 72 bp. The 16S rRNA measures 1410 bp with an AT content of 86.17%, and the 12S rRNA is 785 bp with an AT content of 85.23%. The control region, at 700 bp, shows a strong T skew (AT skew of −0.16) and a pronounced C skew (GC skew of −0.36) (Table 4).

Table 3. Nucleotide composition and skewness of mitogenomes of *Robackia demeijerei* (PCG: Protein-Coding Gene, CR: Control Region).

Gene Type	Length (bp)	Base Composition (%)						Skew	
		A	T	C	G	A + T	G + C	AT-Skew	GC-Skew
Whole genome	16,218	41.61	39.25	7.96	11.18	80.86	19.14	0.03	−0.17
PCG	11,220	33.22	46.16	9.90	10.72	79.38	20.62	−0.16	−0.04
PCG 1st codon position	3740	34.48	39.10	15.62	10.80	73.59	26.41	−0.06	0.18
PCG 2nd codon position	3740	21.61	49.13	11.69	17.57	70.74	29.26	−0.39	−0.20
PCG 3rd codon position	3740	43.57	50.23	2.40	3.80	93.80	6.20	−0.07	−0.23
ATP6	678	34.81	42.63	8.85	13.72	77.44	22.57	−0.10	−0.22
ATP8	168	42.86	44.64	4.17	8.33	87.50	12.50	−0.02	−0.33
COX1	1536	32.10	37.96	14.26	15.69	70.06	29.95	−0.08	−0.05
COX2	684	36.11	40.50	10.38	13.01	76.61	23.39	−0.06	−0.11
COX3	789	30.54	39.04	13.94	16.48	69.58	30.42	−0.12	−0.08
CYTB	1137	32.81	41.07	11.17	14.95	73.88	26.12	−0.11	−0.14
ND1	942	27.71	49.68	14.33	8.28	77.39	22.61	−0.28	0.27
ND2	1029	35.28	49.17	6.22	9.33	84.45	15.55	−0.16	−0.20
ND3	354	35.03	47.74	7.91	9.32	82.77	17.23	−0.15	−0.08
ND4	1338	30.64	50.07	12.33	6.95	80.71	19.28	−0.24	0.28
ND4L	294	25.17	59.18	9.18	6.46	84.35	15.64	−0.40	0.17
ND5	1737	30.63	49.45	11.46	8.46	80.08	19.92	−0.24	0.15
ND6	534	38.20	48.88	4.49	8.43	87.08	12.92	−0.12	−0.30
All rRNA	2248	43.11	43.03	9.24	4.64	86.13	13.88	0.00	0.33
12S	854	44.03	41.57	9.37	5.04	85.60	14.41	0.03	0.30
16S	1394	42.18	44.48	9.11	4.23	86.66	13.34	−0.03	0.37
CR	481	48.23	48.65	1.87	1.25	96.88	3.12	0.00	0.20

Table 4. Nucleotide composition and skewness of mitogenomes of *Saetheria tamanipparai* (PCG: Protein-Coding Gene, CR: Control Region).

Gene Type	Length (bp)	Base Composition (%)						Skew	
		A	T	C	G	A + T	G + C	AT-Skew	GC-Skew
Whole genome	15,899	39.91	39.20	8.40	12.50	79.11	20.90	0.01	−0.20
PCG	11,220	31.60	45.80	10.44	12.16	77.40	22.60	−0.18	−0.08
PCG 1st codon position	3740	32.93	39.61	16.36	11.10	72.54	27.46	−0.09	0.19
PCG 2nd codon position	3740	21.07	48.39	11.91	18.63	69.46	30.54	−0.39	−0.22
PCG 3rd codon position	3740	40.80	49.38	3.05	6.77	90.18	9.82	−0.10	−0.38
ATP6	678	31.27	44.69	8.26	15.78	75.96	24.04	−0.18	−0.31
ATP8	168	36.90	47.02	2.98	13.10	83.92	16.08	−0.12	−0.63
COX1	1536	30.60	38.41	14.71	16.28	69.01	30.99	−0.11	−0.05
COX2	684	33.48	38.89	11.99	15.64	72.37	27.63	−0.07	−0.13
COX3	789	30.80	38.15	13.81	17.24	68.95	31.05	−0.11	−0.11
CYTB	1137	32.10	39.58	11.70	16.62	71.68	28.32	−0.10	−0.17
ND1	942	27.49	49.79	14.12	8.60	77.28	22.72	−0.29	0.24
ND2	1029	33.53	49.37	7.00	10.11	82.90	17.11	−0.19	−0.18
ND3	354	32.49	45.48	8.47	13.56	77.97	22.03	−0.17	−0.23
ND4	1338	28.48	49.25	14.72	7.55	77.73	22.27	−0.27	0.32
ND4L	294	25.51	58.84	9.86	5.78	84.35	15.64	−0.40	0.26
ND5	1737	30.69	47.55	13.07	8.69	78.24	21.76	−0.22	0.20
ND6	534	37.45	48.31	5.06	9.18	85.76	14.24	−0.13	−0.29
All rRNA	2195	43.35	42.36	9.66	4.65	85.70	14.31	0.01	0.35
12S	785	43.57	41.66	9.81	4.97	85.23	14.78	0.02	0.33
16S	1410	43.12	43.05	9.50	4.33	86.17	13.83	0.00	0.37
CR	700	40.14	55.86	1.29	2.71	96.00	4.00	−0.16	−0.36

The ω (Ka/Ks ratio) within the *Harnischia* generic complex, which serves as a gauge for evolutionary sequence rates influenced by natural selection, was consistently found to be less than one across the 13 protein-coding genes (PCGs) analyzed in our study, aligning with patterns observed in other insects. The ω values ranged from a low of 0.044 for *COX1* to a high of 0.441 for *ATP8*, indicating a spectrum of purifying selection intensities. Notably, *ND6* showed the most rapid evolution, while *COX1* was the slowest (Figure 2a). Genes experiencing more stringent purifying selection, such as *COX2* and *COX1*, had lower ω values, whereas *ATP8*, *ND6*, and *ND5* displayed a less stringent selective pressure. These results highlight the significant impact of natural selection on the evolutionary trajectory of PCGs.

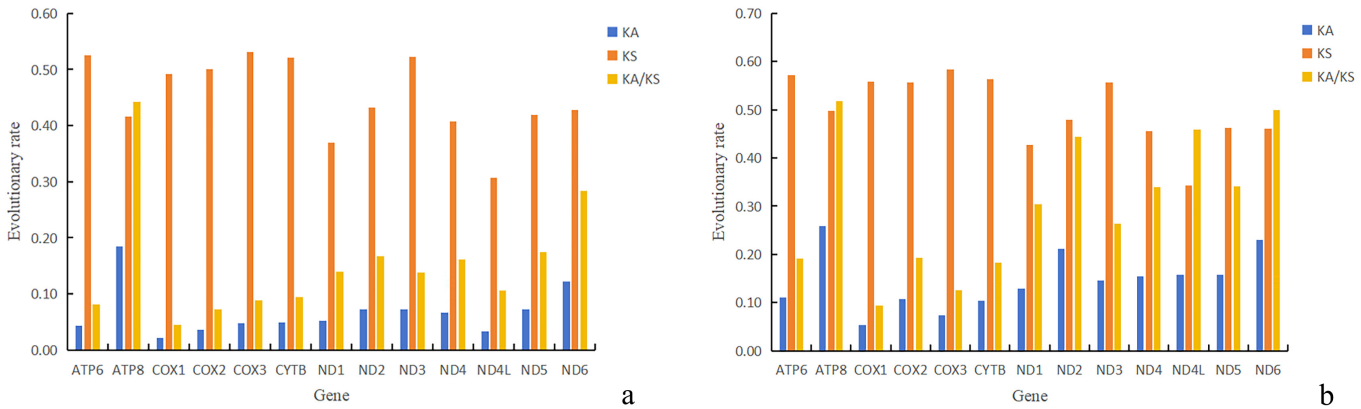

Figure 2. Evolution rate of 13 PCGs of the subfamily Chironominae in mitogenomes, (**a**): *Harnischia* generic complex, (**b**): other genera within Chironominae. Ka and Ks represent non-synonymous and synonymous nucleotide substitutions, respectively, with their ratio, Ka/Ks, indicating the selection pressure on protein-coding genes (PCGs). The plot's x-axis shows 13 PCGs, and the y-axis shows Ka/Ks values.

The Ka/Ks ratio (ω) of other genera in subfamily Chironominae, the Ka/Ks ratio (ω), an indicator of evolutionary sequence rates under the influence of natural selection, was uniformly below one for all 13 protein-coding genes (PCGs) across the genera we examined, echoing the patterns seen in various other insect species. The ω values spanned from a minimum of 0.093 for *COX1* to a maximum of 0.517 for *ATP8*, indicating a gradient of purifying selection pressures. *ATP8* was identified as the gene evolving at the fastest pace, while *COX1* evolved at the slowest rate (Figure 2b). Genes subjected to more intense purifying selection, such as *COX3* and *COX1*, demonstrated lower ω values, in contrast to *ATP8*, *ND6*, and *ND4L*, which showed signs of a more lenient selective regime. These observations underscore the pivotal role that natural selection plays in the evolution of PCGs. The Ka/Ks ratio within the subfamily Chironominae does not exhibit significant variation, with statistical similarities being nearly consistent. Whether within the *Harnischia* complex or other genera of the Chironominae, the lowest ratio is observed in COX1, while the highest is found in ATP8. This pattern is relatively common within the family Chironomidae.

The examination of heterogeneity divergence differences offers insights into the mitochondrial gene sequence similarities among various species. It is worth noting that due to codon degeneracy, the cds_faa dataset exhibited the lowest level of heterogeneity, whereas the cds_rrna dataset demonstrated a notably higher degree of heterogeneity (Figure 3).

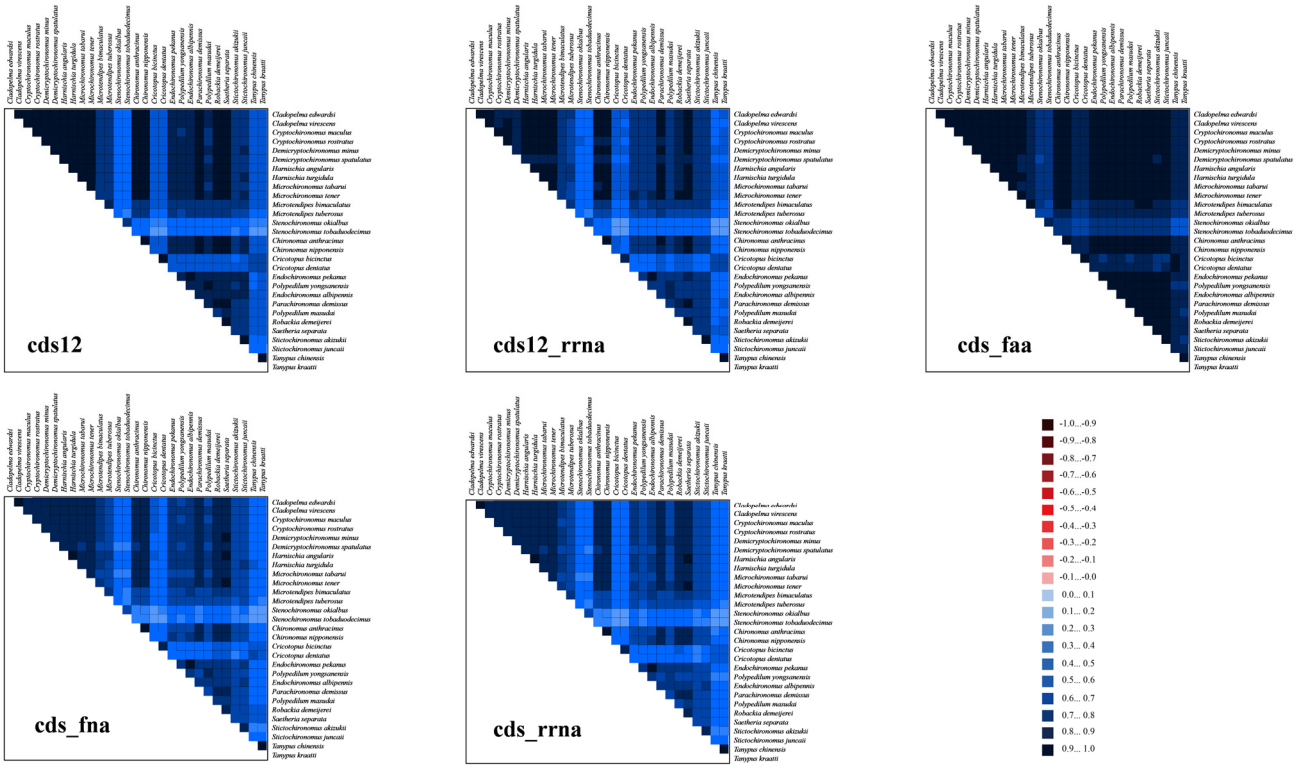

Figure 3. The assessment of the heterogeneity among the mitogenomes of 29 species belonging to the Chironomidae. This figure highlights the sequence similarities among Protein-Coding Genes (PCGs), amino acid sequences, and ribosomal RNAs (rRNAs) through a visually striking color-coded block representation. Utilizing the AliGROOVE scoring system, we assigned colors from −1 (red, denoting high heterogeneity) to +1 (blue, denoting low heterogeneity). The color scheme is such that lighter shades represent increased genetic variability, and deeper tones suggest reduced heterogeneity.

4. Discussion

This finding indicates that the mutation rate for the third codon position in protein-coding genes (PCGs) has exceeded that of the first and second positions. As a result, the third codon positions were deemed inappropriate for inferring the phylogenetic relationships among the three genera. In our research, we leveraged the strengths of Bayesian inference (BI) and maximum likelihood (ML) approaches, employing five different datasets to generate a total of ten phylogenetic trees. Our data revealed that the newly sequenced and assembled species of *Parachironomus demissum*, *Robackia demeijerei*, and *Saetheria tamanipparai* are supported by mitochondrial genome data to belong to Harnischia generic complex, with *Parachironomus* and *Robackia* exhibiting a sister-group relationship (Figure 4).

There is relatively limited and contradictory research on the systematic studies of *Harnischia* generic complex. A tree constructed through TNT (Tree analysis utilizing New Technology), drawing upon 74 female-specific traits, reinforces the sister-group relationship between *Cryptochironomus* and *Demicryptochironomus*, with the reconstructed phylogeny further situating *Harnischia* as the sister to the (*Cryptochironomus* + *Demicryptochironomus*) clade, a perspective corroborated by preliminary mitochondrial genome findings for a selection of these taxa [5,11,18]. Utilizing newly resequenced data in conjunction with already published mitochondrial genome sequences, we conducted a phylogenetic analysis focusing on eight genera within the *Harnischia* generic complex. Our findings once again uphold the sister-group relationship between *Cryptochironomus* and *Demicryptochironomus*. Furthermore, our analysis also confirms the close affinity between (*Cryptochironomus* + *Demicryptochironomus*) and (*Harnischia* + *Microchironomus*), aligning consistently with previous research outcomes [5,11].

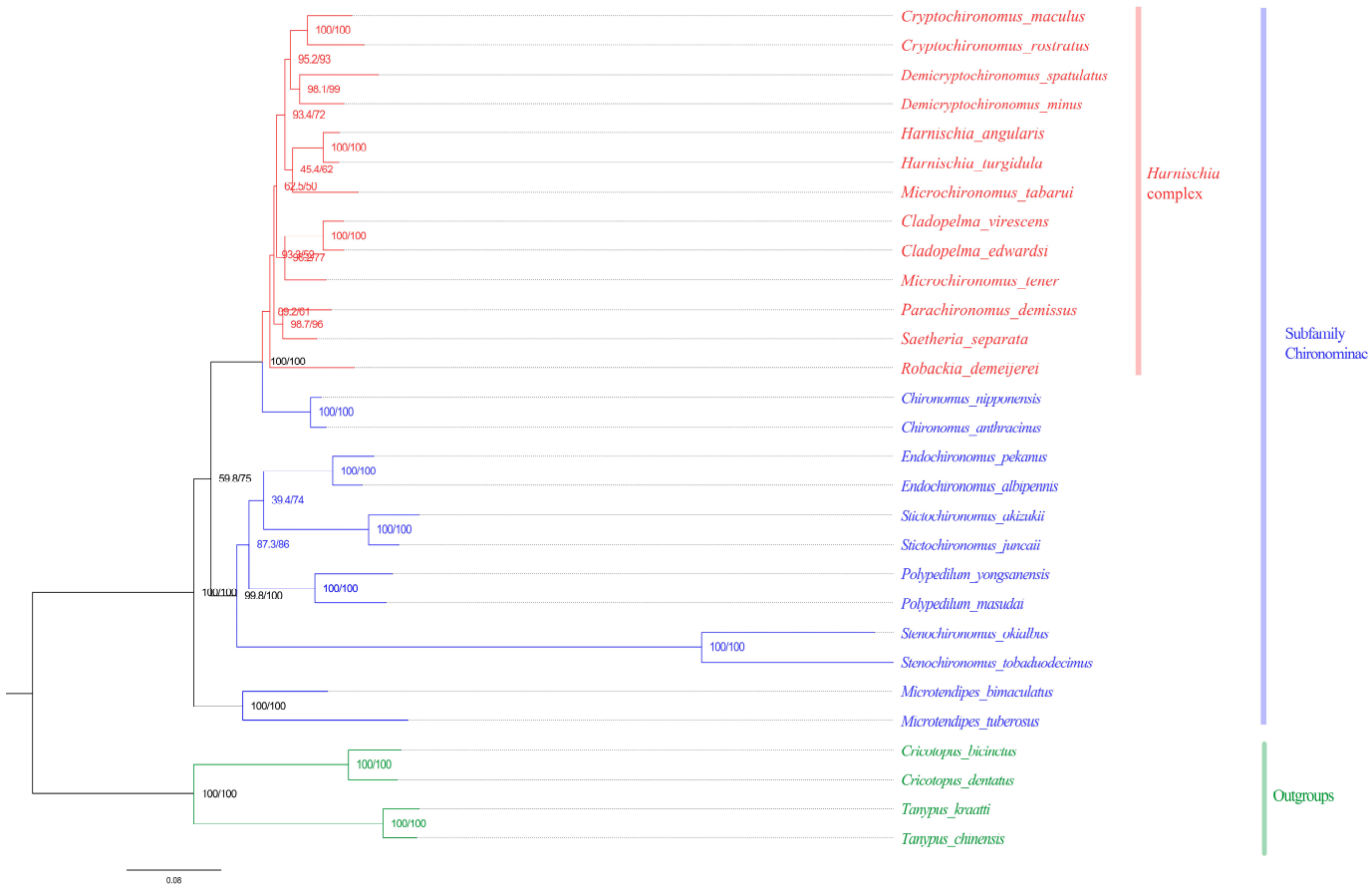

Figure 4. Phylogenetic tree of Chironominae, ML tree based on analysis cds_rRNA in Partition.

Both molecular data from fragments and morphological studies support the sister-group relationship between the *Harnischia* generic complex and the genus *Chironomus* within the Chironomini tribe of Chironomidae [50,51]. Furthermore, the *Harnischia* generic complex and *Chironomus* are phylogenetically close, and their clade forms a sister group with the *Polypedilum* generic complex [51]. Our mitochondrial genome results also corroborate this analysis (Figure 4). Within the *Harnischia* generic complex, morphological data suggest that *Robackia* and *Saetheria* are terminal taxa, relatively evolved, while *Parachironomus* is considered a relatively primitive taxon [51]. However, analysis of fragments of *18SrRNA*, *28SrRNA*, *CAD1*, *CAD4*, and *mtCOI* indicates that *Parachironomus* is a terminal taxon [50]. Based on mitochondrial genome data, *Robackia* is identified as the basal taxon, which is relatively primitive, with *Parachironomus* and *Saetheria* also appearing as primitive within the complex. This represents a novel insight into the phylogeny of the *Harnischia* generic complex, and further species and data are needed in the future to explore more natural phylogenetic relationships within this complex.

5. Conclusions

For the first time, the mitochondrial genomes of three species within the *Harnischia* generic complex were meticulously annotated, assembled, and documented. These newly sequenced mitogenomes exhibit structural features and nucleotide compositions that closely align with those of previously reported Chironomidae species, marking a significant expansion of the Chironomid mitogenome repository. This advancement lays a solid groundwork for future phylogenetic inquiries.

Despite the distinct morphological traits observed among the developmental stages—larvae, pupae, and adult males and females—of different Chironomidae subfamilies, there

is a noted discordance between phylogenetic outcomes based on morphology, short gene sequences, and mitochondrial genome data. However, an emerging consensus from molecular phylogenetics highlights the enduring relevance of morphological analysis in the study of Chironomids. Moreover, while the comprehensive analysis of mitochondrial genomes presents exciting prospects, it necessitates rigorous examination and thoughtful consideration. A holistic systematic analysis that encompasses morphological, biogeographical, and life history traits across various developmental stages of insects, complemented by genomic data, is essential. Such an integrative approach is likely to shed light on the intrinsic evolutionary connections within the natural world.

Supplementary Materials: The following supporting information can be downloaded at: https://www.mdpi.com/article/10.3390/d17020096/s1, Figure S1 depicts the putative secondary structures of the 22 tRNA genes identified within the mitogenome of *Parachironomus demissum*. Figure S2 illustrates the same for *Robackia demeijerei*, while Figure S3 shows the structures for *Saetheria tamanipparai*. Figure S4 presents an ML phylogenetic tree of the subfamily Chironominae based on the cds_faa analysis using the Partition model in IQTREE, with support values indicated by SHaLRT/UFBoot2. Similarly, Figure S5 displays the tree based on the cds analysis, Figure S6 on cds_rrna, and Figure S7 on cds12, all using the same method and support indicators. Figures S8 to S12 present BI phylogenomic trees for the subfamily Chironominae, using the CAT + GTR model in phylobayes. Figure S8 focuses on the cds_faa analysis, Figure S9 on cds, Figure S10 on cds_rrna, Figure S11 on cds12, and Figure S12 on a combined cds12_rrna analysis.

Author Contributions: Conceptualization, W.L. (Wenbin Liu) and Y.T.; Software, Y.T. and J.N.; Investigation, H.Y., W.L. (Wentao Liang) and Y.Z.; Data curation, Y.T., W.L. (Wenbin Liu) and H.Y. Writing—original draft, W.L. (Wenbin Liu), Y.T. and J.N.; Writing—review and editing, C.Y., W.L. (Wentao Liang) and Y.Z.; Supervision, C.Y.; Funding acquisition, W.L. (Wenbin Liu) and C.Y. All authors have read and agreed to the published version of the manuscript.

Funding: This research was funded by the Yinshanbeilu Grassland Ecohydrology National Observation and Research Station, China Institute of Water Resources and Hydropower Research, Beijing 100038, China, Grant NO. YSS202308 and the National Natural Science Foundation of China (32370489, 32170473).

Institutional Review Board Statement: Not applicable.

Data Availability Statement: The original contributions presented in this study are included in the article and Supplementary Material. Further inquiries can be directed to the corresponding author.

Acknowledgments: We thank Xinyu Ge (Tianjin Normal University) for providing assistance with data analysis.

Conflicts of Interest: The authors declare no conflicts of interest.

References

1. Armitage, P.; Cranston, P.; Pinder, C. *The Chironomidae. Biology and Ecology of Non-Biting Midges*; Chapman & Hall: London, UK, 1995; 572p.
2. Liu, W.; Chang, T.; Zhao, K.; Sun, X.; Qiao, H.; Yan, C.; Wang, Y. Genome-wide annotation of cuticular protein genes in non-biting midge *Propsilocerus akamusi* and transcriptome analysis of their response to heavy metal pollution. *Int. J. Biol. Macromol.* **2022**, *223*, 555–566. [CrossRef] [PubMed]
3. Song, C.; Chen, G.; Wang, L.; Lei, T.; Qi, X. DNA Barcoding Supports "Color-Pattern"-Based Species of *Stictochironomus* from China (Diptera: Chironomidae). *Insects* **2024**, *15*, 179. [CrossRef] [PubMed]
4. Ferrington, L.C. Global diversity of non-biting midges (Chironomidae; Insecta-Diptera) in freshwater. *Hydrobiologia* **2008**, *595*, 447–455. [CrossRef]
5. Liu, W.; Wang, C.; Wang, J.; Tang, Y.; Pei, W.; Ge, X.; Yan, C. Phylogenetic and Comparative Analysis of *Cryptochironomus*, *Demicryptochironomus* and *Harnischia* Inferred from Mitogenomes (Diptera: Chironomidae). *Insects* **2024**, *15*, 642. [CrossRef] [PubMed]

6. Lin, X.L.; Liu, Z.; Yan, L.P.; Duan, X.; Bu, W.J.; Wang, X.H.; Zheng, C.G. Mitogenomes provide new insights of evolutionary history of Boreheptagyiini and Diamesini (Diptera: Chironomidae: Diamesinae). *Ecol. Evol.* **2022**, *12*, e8957. [CrossRef] [PubMed]
7. Zhang, D.; He, F.X.; Li, X.B.; Aishan, Z.; Lin, X.L. New Mitogenomes of the *Polypedilum* Generic Complex (Diptera: Chironomidae): Characterization and Phylogenetic Implications. *Insects* **2023**, *14*, 238. [CrossRef]
8. Pinder, L.C.V.; Reiss, F. The pupae of Chironominae (Diptera: Chironomidae) of the Holarctic region—Keys and diagnoses. *Chironomidae of the Holarctic Region. Keys and Diagnoses. Part 2—Pupae*. Wiederholm, T., Ed.; Entomologica scandinavica Supplement 28. 1986, pp. 299–456. Available online: https://www.researchgate.net/publication/382851295_Chironomidae_of_the_Holarctic_region_Keys_and_diagnoses_Part_2_Pupae_Chapters_1_to_9 (accessed on 1 January 2025).
9. Cranston, P.S.; Dillon, M.E.; Pinder, C.V.; Reiss, F. The adult males of Chironominae (Diptera: Chironomidae) of the Holarctic region—Keys and diagnoses. *Chironomidae of the Holarctic Region. Keys and Diagnoses. Part 3. Adult Males*. Wiederholm, T., Ed.; Entomologica scandinavica Supplement 34. 1989, pp. 353–532. Available online: https://www.pemberleybooks.com/product/chironomidae-of-the-holarctic-region.-keys-and-diagnoses.-part-3.-adult-males-entomologica-scandinavica-supplement-34/7156/ (accessed on 1 January 2025).
10. Armitage, P.D.; Pinder, L.; Cranston, P. *The Chironomidae: Biology and Ecology of Non-Biting Midges*; Springer Science & Business Media: Berlin/Heidelberg, Germany, 2012.
11. Sæther, O.A. Female genitalia in Chironomidae and other Nematocera: Morphology, phylogenies, keys. *Bull. Fish. Res. Bd. Can.* **1977**, *197*, 1–209.
12. Orel, O.V.; Kang, H.J.; Makarchenko, E.A. Non-biting midges of the tribe Chironomini (Diptera: Chironominae) from North Korea. *Far East. Ent.* **2017**, *331*, 1–16.
13. Mukherjee, B.; Hazra, N. Taxonomic studies on *Harnischia* complex from India (Diptera: Chironomidae). *Zootaxa* **2023**, *5278*, 239–263. [CrossRef]
14. Yan, C. Systematic Study of the *Harnischia* Generic Group (Diptera: Chironomidae) in the China-India Region. Ph.D. Thesis, Nankai University, Tianjin, China, 2007.
15. Beck, E.C.; Beck, W.M. Chironomidae (Diptera) of Florida III. The *Harnischia* complex (Chironiominae). University of Florida Gainesville. Bulletin of the Florida State Museum. *Biol. Sci.* **1969**, *13*, 277–313.
16. Townes, H.K. The Nearctic species of Tendipedini (Diptera; Tendipedidae (= Chironomidae)). *Am. Midl. Nat.* **1945**, *34*, 1–206. [CrossRef]
17. Sæther, O.A. Taxonomic studies on Chironomidae: *Nanocladius*, *Pseudochironomus*, and the *Harnischia* complex. *Bull. Fish. Res. Bd Can.* **1977**, *196*, 1–143.
18. Sæther, O.A. Phylogeny of the subfamilies of Chironomidae (Diptera). *Syst. Entomol.* **2000**, *25*, 393–403. [CrossRef]
19. Cameron, S.L. Insect mitochondrial genomics: Implications for evolution and phylogeny. *Annu. Rev. Entomol.* **2014**, *59*, 95–117. [CrossRef] [PubMed]
20. Zheng, B.; Han, Y.; Yuan, R.; Liu, J.; Tang, P.; van Achterberg, C.; Chen, X. Mitochondrial Genomes Yield Insights into the Basal Lineages of Ichneumonid Wasps (Hymenoptera: Ichneumonidae). *Genes* **2022**, *13*, 218. [CrossRef] [PubMed]
21. Boore, J.L. Animal mitochondrial genomes. *Nucleic Acids Res.* **1999**, *27*, 1767–1780. [CrossRef] [PubMed]
22. Zhang, L.J.; Li, Y.J.; Ge, X.Y.; Li, X.Y.; Yang, Y.X.; Bai, M.; Ge, S.Q. Mitochondrial genomes of *Sternochetus* species (Coleoptera: Curculionidae) and the phylogenetic implications. *Arch. Insect. Biochem.* **2022**, *111*, e21898. [CrossRef] [PubMed]
23. Chen, Z.T.; Du, Y.Z. Comparison of the complete mitochondrial genome of the stonefly *Sweltsa longistyla* (Plecoptera: Chloroperlidae) with mitogenomes of three other stoneflies. *Gene* **2015**, *558*, 82–87. [CrossRef] [PubMed]
24. Ge, X.; Zang, H.; Ye, X.; Peng, L.; Wang, B.; Lian, G.; Sun, C. Comparative Mitogenomic Analyses of Hydropsychidae Revealing the Novel Rearrangement of Protein-Coding Gene and tRNA (Trichoptera: Annulipalpia). *Insects* **2022**, *13*, 759. [CrossRef]
25. Ge, X.; Peng, L.; Vogler, A.P.; Morse, J.C.; Yang, L.; Sun, C.; Wang, B. Massive gene rearrangements of mitochondrial genomes and implications for the phylogeny of Trichoptera (Insecta). *Syst. Entomol.* **2023**, *48*, 278–295. [CrossRef]
26. Li, X.Y.; Yan, L.P.; Pape, T.; Gao, Y.Y.; Zhang, D. Evolutionary insights into *bot flies* (Insecta: Diptera: Oestridae) from comparative analysis of the mitochondrial genomes. *Int. J. Biol. Macromol.* **2020**, *149*, 371–380. [CrossRef] [PubMed]
27. Ge, X.; Wang, J.; Zang, H.; Chai, L.; Liu, W.; Zhang, J.; Yan, C.; Wang, B. Mitogenomics Provide New Phylogenetic Insights of the Family Apataniidae (Trichoptera: Integripalpia). *Insects* **2024**, *15*, 973. [CrossRef]
28. Lin, X.; Zhao, Y.; Yan, L.; Liu, W.; Bu, W.; Wang, X.; Zheng, C. Mitogenomes provide new insights into the evolutionary history of Prodiamesinae (Diptera: Chironomidae). *Zool. Scr.* **2021**, *51*, 119–132. [CrossRef]
29. Li, S.; Chen, M.; Sun, L.; Wang, R.; Li, C.; Gresens, S.; Li, Z.; Lin, X. New mitogenomes from the genus *Cricotopus* (Diptera: Chironomidae, Orthocladiinae): Characterization and phylogenetic implications. *Arch. Insect Biochem. Physiol.* **2023**, *115*, e22067. [CrossRef] [PubMed]
30. Qi, Y.; Bu, W.; Zheng, C.; Lin, X.; Jiao, K. New data on mitogenomes of *Thienemanniella* Kieffer, 1911 (Diptera: Chironomidae, Orthocladiinae). *Arch. Insect Biochem. Physiol.* **2023**, *114*, 1–9. [CrossRef]

31. Gao, S.; Wang, C.; Tang, Y.; Zhang, Y.; Ge, X.; Zhang, J.; Liu, W. Complete Mitochondrial Genome of *Tanypus chinensis* and *Tanypus kraatzi* (Diptera: Chironomidae): Characterization and Phylogenetic Implications. *Genes* **2024**, *15*, 1281. [CrossRef]
32. Andersen, T.; Ekrem, T.; Cranston, P.S. The larvae of the Holarctic Chironomidae (Diptera)—Introduction. *Insect Syst. Evol. Suppl.* **2013**, *66*, 7–12.
33. Epler, J.H. Identification manual for the larval Chironomidae (Diptera) of North and South Carolina. Version 1.0. St. Johns Riv. Wat. Mgmt Distr. Spec. Publ. SJ2001-SP13, FL. 2001, pp. vi + 516. Available online: https://johnepler.com/SEMidges.pdf (accessed on 1 January 2025).
34. Liu, W.B.; Wang, Y.; Zhao, K.Z.; Wang, C.Y.; Zhang, J.Y.; Yan, C.C.; Lin, X.L. New species, a new combination, and DNA barcodes of *Parachironomus* Lenz, 1921 (Diptera, Chironomidae). *ZooKeys* **2023**, *1153*, 121–140. [CrossRef] [PubMed]
35. Yan, C.; Sæther, O.A.; Wang, X. Saetheria Jackson from the Sino-Indian Region (Diptera: Chironomidae). *Zootaxa* **2011**, *3040*, 34–42. [CrossRef]
36. Yan, C.; Wang, X.; Bu, W. A new species in the genus *Paracladopelma* Harnisch (Diptera: Chironomidae) from China. *Entomotaxonomia* **2012**, *34*, 291–295.
37. Yan, C.; Wang, X. *Robackia* Sæther from China (Diptera: Chironomidae). *Zootaxa* **2006**, *1361*, 53–59. [CrossRef]
38. Bolger, A.; Lohse, M.; Usadel, B. Trimmomatic: A flexible trimmer for Illumina sequence data. *Bioinformatics* **2014**, *30*, 2114–2120. [CrossRef]
39. Dierckxsens, N.; Mardulyn, P.; Smits, G. NOVOPlasty: De novo assembly of organelle genomes from whole genome data. *Nucleic Acids Res.* **2016**, *45*, e18. [CrossRef]
40. Katoh, K.; Standley, D.M. MAFFT Multiple Sequence Alignment Software Version 7: Improvements in Performance and Usability. *Mol. Biol. Evol.* **2013**, *30*, 772–780. [CrossRef] [PubMed]
41. Kumar, S.; Stecher, G.; Tamura, K. MEGA7: Molecular Evolutionary Genetics Analysis Version 7.0 for Bigger Datasets. *Mol. Biol. Evol.* **2016**, *33*, 1870–1874. [CrossRef] [PubMed]
42. Shen, W.; Le, S.; Li, Y.; Hu, F. SeqKit: A Cross-Platform and Ultrafast Toolkit for FASTA/Q File Manipulation. *PLoS ONE* **2016**, *11*, e0163962. [CrossRef] [PubMed]
43. Tamura, K.; Stecher, G.; Kumar, S. MEGA11: Molecular Evolutionary Genetics Analysis Version 11. *Mol. Biol. Evol.* **2021**, *38*, 3022–3027. [CrossRef]
44. Rozas, J.; Ferrer-Mata, A.; Sánchez-DelBarrio, J.C.; Guirao-Rico, S.; Librado, P.; RamosOnsins, S.E.; Sánchez-Gracia, A. DnaSP 6: DNA Sequence Polymorphism Analysis of Large Data Sets. *Mol. Biol. Evol.* **2017**, *34*, 3299–3302. [CrossRef] [PubMed]
45. Capella-Gutiérrez, S.; Silla-Martínez, J.; Gabaldón, T. trimAl: A tool for automated alignment trimming in large-scale phylogenetic analyses. *Bioinformatics* **2009**, *25*, 1972–1973. [CrossRef] [PubMed]
46. Kück, P.; Meid, S.A.; Groß, C.; Wägele, J.W.; Misof, B. AliGROOVE—Visualization of heterogeneous sequence divergence within multiple sequence alignments and 6 detection of inflated branch support. *BMC Bioinform.* **2014**, *15*, e294. [CrossRef]
47. Li, S.-Y.; Zhao, Y.-M.; Guo, B.-X.; Li, C.-H.; Sun, B.-J.; Lin, X.-L. Comparative Analysis of Mitogenomes of *Chironomus* (Diptera: Chironomidae). *Insects* **2022**, *13*, 1164. [CrossRef]
48. Zheng, C.-G.; Liu, Z.; Zhao, Y.-M.; Wang, Y.; Bu, W.-J.; Wang, X.-H.; Lin, X.-L. First Report on Mitochondrial Gene Rearrangement in Non-Biting Midges, Revealing a Synapomorphy in *Stenochironomus* Kieffer (Diptera: Chironomidae). *Insects* **2022**, *13*, 115. [CrossRef] [PubMed]
49. Kong, F.-Q.; Zhao, Y.-C.; Chen, J.-L.; Lin, X.-L. First report of the complete mitogenome of *Microchironomus tabarui* Sasa, 1987 (Diptera, Chironomidae) from Hebei Province, China. *Mitochondrial DNA Part B* **2021**, *6*, 2845–2846. [CrossRef]
50. Cranston, P.; Hardy, N.; Morse, G. A dated molecular phylogeny for the Chironomidae (Diptera). *Syst. Entomol.* **2011**, *37*, 172–188. [CrossRef]
51. Andersen, T.; Mendes, H.F.; Pinho, L.C. Two new Neotropical Chironominae genera (Diptera: Chironomidae). *Chironomus J. Chironomidae Res.* **2017**, *30*, 26–54. [CrossRef]